

Infrared Reflection Spectra of $\text{Ga}_{1-x}\text{Al}_x\text{As}$ Mixed Crystals*

M. ILEGEMST† AND G. L. PEARSON

Stanford Electronics Laboratories, Stanford University, Stanford, California 94035

(Received 22 September 1969)

The infrared lattice-vibration spectra of $\text{Ga}_{1-x}\text{Al}_x\text{As}$ mixed crystals have been studied by measuring the room-temperature reflectivity at near-normal incidence in the 200–600- cm^{-1} frequency range. Two distinct reststrahlen bands with frequencies near those of pure GaAs and pure AlAs were observed over the entire composition range investigated. Each band shifts to lower frequencies and decreases in amplitude as the concentration of the corresponding compound in the alloy is decreased. An analysis of the data using the Kramers-Kronig technique and classical dispersion theory gives the transverse and longitudinal mode frequencies. The changes of these mode frequencies with composition are interpreted on the basis of the random-element isodisplacement model.

I. INTRODUCTION

THIS paper reports measurements of the reflection spectra of $\text{Ga}_{1-x}\text{Al}_x\text{As}$ mixed crystals in the infrared reststrahlen region. Throughout the composition range $x=0.08$ – 0.82 investigated here, the reflectivity spectra show two distinct bands, one at a frequency close to the optical-phonon mode of pure GaAs, the other near the mode frequency of pure AlAs. The strength and frequency of each mode depend on composition. Specifically, both the AlAs-like and the GaAs-like bands shift slightly to lower frequencies and decrease in amplitude when the concentrations of, respectively, Al and Ga in the alloy are reduced. The experimental results are presented in Sec. II

Two-mode behavior has been reported previously in other III–V compound mixed crystals with group-V element substitution such as $\text{GaAs}_x\text{P}_{1-x}$.^{1,2} Of the mixed crystals with group-III element substitution, $\text{Ga}_{1-x}\text{Al}_x\text{As}$ is the first to display a two-mode behavior at all compositions, since in the only other such system studied to date, $\text{Ga}_x\text{In}_{1-x}\text{As}$, a particular type of response was found in which the GaAs-like and the InAs-like bands merge into a single reststrahlen band at the InAs-rich end of the composition range.³ The conditions for the occurrence of one- or two-mode behavior are reasonably well understood on the basis of local-mode theory. The criteria for two-band behavior are that, in the heavier ion compound, the local mode due to the substituted ion must fall above the optical branch of the host crystal spectrum and that, similarly, in the lighter ion compound, the substituted impurity ion must give rise either to a localized gap mode between the acoustical and optical branches of the parent crystal, or to an in-band resonance mode. This suggests that two bands will appear only in those mixed systems

in which the reststrahlen bands of the pure compounds are well separated and in which, near the ends of the composition range, the local or impurity resonance mode of the minority ion lies well outside the main resonance mode of the parent crystal. The experimental results presented here indicate that both of these conditions are satisfied in the AlAs–GaAs system.

The $\text{Ga}_{1-x}\text{Al}_x\text{As}$ system is of special interest for studying the composition dependence of the optical-phonon frequencies since the lattice mismatch between the two end compounds is extremely small so that the substitutional solid solutions can be considered as ideal and nearly free of stress. As a result, the distribution of Ga and Al ions within the group-III sublattice is expected to be essentially random. This observation is corroborated by the fact that little or no fine structure, which may result from microscopic scale clustering in the lattice, is observed in the measured reflectance spectra. In Sec. III, the transverse-optical (TO) and longitudinal-optical (LO) frequencies of both the GaAs-like and the AlAs-like modes are determined at each composition by means of a Kramers-Kronig dispersion analysis of the spectra, and the frequency of each band is traced throughout the composition range from the region where the band forms the dominant lattice mode to the region where the band reduces to an impurity mode.

Finally, in Sec. IV, the experimental results are analyzed and the shifts of the TO and LO mode frequencies with composition interpreted on the basis of the random-element-isodisplacement (REI) model⁴ with two infrared active modes. When the original model equations are expanded by including effective charge terms accounting for local-field coupling and by allowing the first-neighbor force constants to be composition-dependent, a reasonably good agreement between model and experiment is obtained. The values of the model parameters indicate that both the Al-As and the Ga-As bond strengths carry an important ionic contribution and that the strength of the Ga-As bond increases with decreasing Ga concentration in the alloy.

* Work supported by USAECOM Night Vision Laboratory, Fort Belvoir, Va. and by the Advanced Research Projects Agency through the Center for Materials Research at Stanford University.

† Present address: Bell Telephone Laboratories, Murray Hill, N. J.

¹ Y. S. Chen, W. Shockley, and G. L. Pearson, *Phys. Rev.* **151**, 648 (1966).

² H. W. Verleur and A. S. Barker, *Phys. Rev.* **149**, 715 (1966).

³ M. H. Brodsky and G. Lucovsky, *Phys. Rev. Letters* **21**, 990 (1968).

II. EXPERIMENT

A. Materials Preparation

All of the mixed crystals used in this study were grown in this laboratory by liquid-phase epitaxy on (111) oriented GaAs substrates.⁴ Thickness of the grown layers varied between 50 and 100 $m\mu$ depending on the melt composition and the temperature interval during growth. Sample areas ranged from 8 to 50 mm^2 . Crystal compositions were determined by electron-beam probing for five of the mixed crystal samples, whereas the compositions of three other mixed crystals were estimated from the position of the short-wavelength reflectivity minimum in the spectra, as discussed in Sec. II C. As a result of the growth technique, the composition of the layers varied slightly with depth. The total change in composition over the thickness of the layers is estimated at less than 2%. The pure single-crystal GaAs crystals were obtained from the Monsanto Co. The AlAs material was grown in our laboratory in a closed evacuated ampoule by reaction of Al and As vapors to form a polycrystalline film. Surface preparation for the GaAs and mixed crystal samples consisted of polishing with a 0.3- $m\mu$ alumina abrasive. The samples containing low Al concentrations were polished mechanically, but those of high Al content had to be polished by hand under methanol to prevent hydrolysis. As a consequence, the surface finish varied to some extent with sample composition and degraded as the AlAs concentration increased. The pure AlAs material was used as grown. All materials were undoped and had carrier concentrations, except for the AlAs sample which could not be measured in the low 10^{16} cm^{-3} range.

B. Reflectivity Measurements

The reflection spectra were obtained with a Perkin Elmer 621 grating infrared spectrophotometer equipped with a 221-0357 specular-reflectance attachment. The angle of incidence of the radiation was 13° . The spectra were first recorded automatically in the region from 600 to 200 cm^{-1} and data were then tabulated point by point in the zones of interest. Wavenumber calibration is better than 0.5 cm^{-1} and the spectral-slit width was less than 4 cm^{-1} over the entire frequency range. All mixed crystal spectra were measured without removing the grown layer from the substrate.

Absolute reflectance values could be obtained with good accuracy only on the large-area samples. The main source of experimental error is expected to result from differences in surface finish between samples, since in the reststrahlen band the reflectivity may be strongly surface-dependent.⁵ For some of the smaller samples, and for the AlAs sample, only relative reflectance

values could be obtained. In order to allow meaningful comparisons to be made, these spectra were normalized by multiplying all reflectivity values by a constant factor. These normalizing factors were chosen such that the reflectance values at the high-frequency limit of the spectra, 600 cm^{-1} , interpolated smoothly between values measured on samples with adjacent compositions.

C. Experimental Results

The reflectivity spectra obtained on seven samples ranging in composition from pure GaAs to pure AlAs are shown in Fig. 1. Other samples measured but not shown displayed similar characteristics. Typical two-mode behavior is observed at all mixed crystal compositions. The AlAs-like band remains well defined at all compositions and shifts to slightly lower frequencies with decreasing values of x . The GaAs-like band shifts to lower frequencies but broadens out and falls off sharply in intensity with decreasing values of $1-x$. These results suggest that while Al shows pure local-mode behavior in GaAs, a Ga impurity forms an in-band resonance mode in the AlAs host crystal. Local-mode

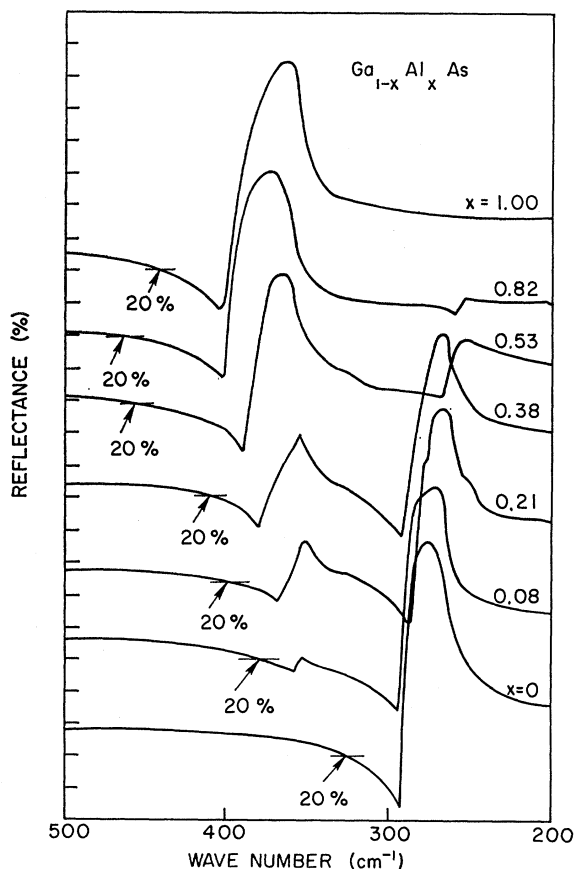


FIG. 1. Normalized reflectance spectra for GaAs, AlAs, and five $\text{Ga}_{1-x}\text{Al}_x\text{As}$ mixed crystals. The curves and their ordinate scales have been displaced for clarity. The ordinate axis is graduated in 10% reflectance intervals.

⁴ M. Ilegems and G. L. Pearson, in *Proceedings of the 1968 Symposium on GaAs* (Institute of Physics and Physical Society, London, 1969), p. 3.

⁵ A. S. Barker, *Phys. Rev.* **132**, 1474 (1963).

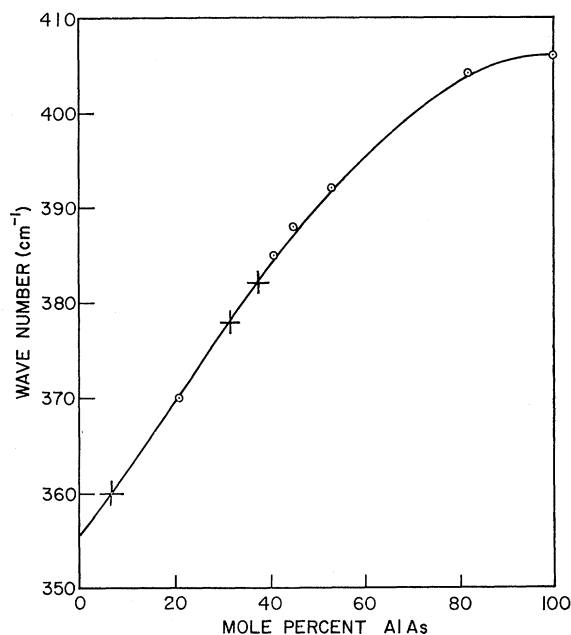


FIG. 2. Position of the short-wavelength reflectivity minimum versus alloy composition. The curve is a smooth line drawn through the data points (○) for which the sample composition was determined by electron-beam probing. The graph was used to determine the composition of three other samples (+) listed in Table I.

absorption of Al in GaAs has been reported by Lorimor *et al.*⁶

A marked feature of the spectra is the large shift in frequency of the short-wavelength reflectivity minimum from its position at 406 cm^{-1} for pure AlAs to 360 cm^{-1} for the sample with the lowest Al content. This concentration dependence is shown in Fig. 2. Over the entire composition range from pure GaAs to pure AlAs, the frequency shift amounts to approximately 50 cm^{-1} . Since the location of the minimum can be established to better than $\pm 1 \text{ cm}^{-1}$, the sample composition can be determined from the spectra to an accuracy of $\pm 2\%$ (absolute). This accuracy is comparable to or better than that obtained by electron-beam probing which is the technique usually used in the GaAs-AlAs system where the lattice mismatch is too small to allow determination of composition from lattice-parameter values.

III. ANALYSIS OF EXPERIMENTAL SPECTRA

A. Determination of Mode Frequencies

The frequencies of the resonant LO and TO modes were obtained from a Kramers-Kronig analysis of the spectra shown in Fig. 1. The Kramers-Kronig integral extends formally from zero to infinity and permits the determination of the optical constants n and k , or, alternatively, ϵ_1 and ϵ_2 , at each frequency from a

⁶ O. G. Lorimor, W. G. Spitzer, and M. Waldner, J. Appl. Phys. **37**, 2509 (1966).

knowledge of the reflectivity spectrum only. In the analysis of the lattice vibration spectra, however, reflectivity values are required only in the energy regions containing and immediately surrounding the reststrahlen bands, since the contribution of the lattice to the total reflectivity levels off to constant values at frequencies far above and below the reststrahlen regions. In this study, between 40 and 100 data points, covering the energy range from 200 to 600 cm^{-1} , were tabulated for each recorded spectrum and introduced in a computer program performing the Kramers-Kronig transform of the reflectivity data. The program assumes constant reflectivity in the frequency regions from 0 to 200 cm^{-1} and from 600 cm^{-1} upward to higher energies. The computer output lists the values of n , k , ϵ_1 , ϵ_2 , and $\text{Im}(1/\epsilon)$ (the energy loss function) at each datum point. In the analysis of the mixed crystal spectra, both ϵ_2 and $\text{Im}(1/\epsilon)$ show two sharp maxima without detectable fine structure. The frequencies of these maxima are taken to correspond, respectively, to the TO phonon frequencies ω_t and to the LO phonon frequencies ω_l .

Figure 3 shows the variation of these LO and TO mode frequencies with alloy composition. The numerical data are tabulated in Table I. The subscripts 1 and 2 indicate AlAs-like and GaAs-like modes, respectively. The accuracy with which the LO and TO frequencies can be obtained from the Kramers-Kronig analysis is estimated to be better than $\pm 2 \text{ cm}^{-1}$. In order to check the validity of the Kramers-Kronig procedure, a classical oscillator fit to the $x=0.82$ spectrum was performed in the 300–600 cm^{-1} frequency range by taking ω_t , ω_l , and γ (the damping coefficient) as adjust-

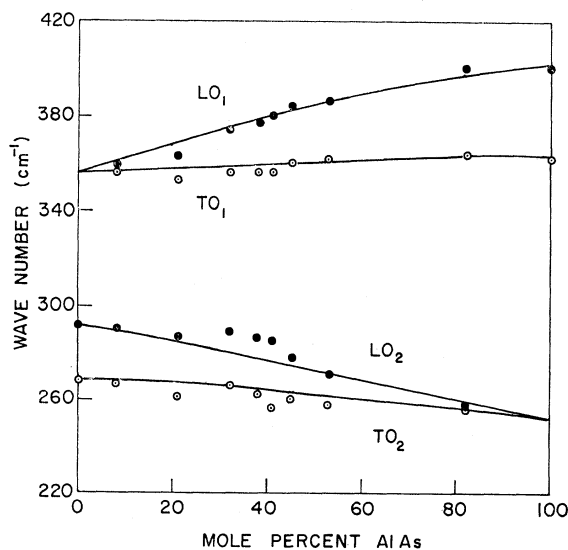


FIG. 3. TO and LO mode frequencies, as obtained from a Kramers-Kronig analysis of the mixed crystal spectra, plotted versus alloy composition. The solid lines are calculated from the REI model (see text).

TABLE I. Mode frequencies obtained from the Kramers-Kronig analysis of the reflectivity spectra.

x	ω_{11} (cm^{-1})	ω_{11} (cm^{-1})	ω_{12} (cm^{-1})	ω_{12} (cm^{-1})
0	268	292
0.08	356	359	267	291
0.21	352	362	260	286
0.32	356	374	266	290
0.38	356	377	262	288
0.41	356	380	256	286
0.45	360	384	260	278
0.53	362	386	258 ^a	270 ^a
0.82	365	400	256 ^a	258 ^a
1.00	362	400

^a At these concentrations, ω_{12} and ω_{22} could not be determined from the Kramers-Kronig analysis with sufficient resolution. The values listed are, respectively, the frequencies of the maximum and the minimum of the corresponding reststrahlen band in the spectra.

able parameters.⁷ The value $\epsilon_\infty=8.5$ was adopted for the high-frequency dielectric constant as determined by fitting the measured reflectivity at 600 cm^{-1} for this sample. The best classical oscillator fit to the high-reflectivity band as judged by a least-squares analysis and by visual inspection was obtained for the following set of values: $\omega_t=364\text{ cm}^{-1}$, $\omega_l=400\text{ cm}^{-1}$, and $\gamma=0.02\text{ cm}^{-1}$. The fit is quite insensitive to the value adopted for the dielectric constant. Similar oscillator fits were made to other mixed crystal spectra and the best fit values for the mode frequencies were again found to be in good agreement with those determined by the Kramers-Kronig analysis. A fit to the pure AlAs spectrum was not attempted because of poor sample quality. It is felt that the TO mode frequency obtained for the $x=0.82$ sample should be very close to that of pure AlAs, and it is estimated that the values $\omega_t(\text{AlAs})=364\pm 1\text{ cm}^{-1}$ and $\omega_l(\text{AlAs})=402\pm 1\text{ cm}^{-1}$ are the best available to date. These values may be compared to previous 77°K values obtained from emittance studies⁸ which are, respectively, $\omega_t(\text{AlAs})=371\text{ cm}^{-1}$ and $\omega_l(\text{AlAs})=395\text{ cm}^{-1}$.

For the local mode frequency of Al in GaAs, extrapolation of our data relevant to the sample with the lowest AlAs concentration leads to a value of $\omega_{\text{loc}}(\text{Al})=356\pm 2\text{ cm}^{-1}$. Previously reported for this local mode frequency obtained from infrared absorption studies⁶ were 362 and 359 cm^{-1} at 77 and 300°K , respectively. The difference between the room-temperature values obtained by reflection and absorption techniques exceeds that expected from experimental errors. Since the precision with which the position of the absorption maxima was determined at room temperature is unknown, preference was given to our value in subsequent calculations. The location of the Ga impurity resonance mode in AlAs cannot be determined with similar accuracy from our data since the intensity of the Ga-like

band falls off sharply at low Ga concentrations. The value $\omega_{\text{loc}}(\text{Ga})=252\text{ cm}^{-1}$ was adopted for the calculations in Sec. IV B.

B. Interpretation of Mode-Frequency Shifts

No first-principle theories exist to describe the lattice vibration spectra of mixed crystals although several different models have been proposed and used successfully to interpret the data obtained from measurements on a wide range of mixed crystal materials. For III-V compound mixed crystals, both the REI model proposed by Chen, Shockley, and Pearson¹ and the basic-units model proposed by Verleur and Barker² have been used. These models are alike in that they both assume that nearest-neighbor interactions (Al-As and Ga-As in this alloy) dominate and that the second nearest-neighbor interaction (Al-Ga) is responsible for the frequency shifts of the resonant modes with composition. The models differ in the number of coordinates assigned to the lattice vibration modes. In the REI model, all ions of like species are assumed to vibrate with equal amplitude and phase so that the motion of the lattice is described completely with three coordinates.

The REI representation yields spectra with two infrared-active reststrahlen bands. In the case of $\text{Ga}_{1-x}\text{Al}_x\text{As}$, these bands correspond to the vibrations of the Ga and Al sublattices against the As sublattice, respectively. In the basic-units model, 13 coordinates are allowed for the vibrational modes as suggested by considering all possible nearest-neighbor configurations in the lattice. With this large number of degrees of freedom, the model can account for fine structure in the spectra. However, an additional clustering effect must often be assumed in order to make a good fit with the data. It has not been established whether the eventual existence of clusters in some mixed crystal material may be a result of the growth procedures or may be an intrinsic materials property. Since little or no definite fine structure was detected in the $\text{Ga}_{1-x}\text{Al}_x\text{As}$ mixed crystal spectra, the REI model should be appropriate to provide a good description to the experimental results. In Sec. IV, the mode-frequency variations as a function of composition are computed from this model and compared with the experimental data.

IV. APPLICATION OF REI MODEL

A. Basic Model Equations

These equations have been derived in the literature¹ for the long-wavelength ($k \rightarrow 0$) transverse vibrations, and their application to different mixed crystal systems has been reviewed recently by Barker.⁹ They are reproduced here for reference.

⁹ A. S. Barker, in *Localized Excitations in Solids*, edited by R. F. Wallis (Plenum Publishing Corp., New York, 1968), p. 581.

⁷ W. G. Spitzer, D. Kleinman, and D. Walsh, *Phys. Rev.* **113**, 127 (1959).

⁸ D. L. Stierwalt and R. F. Potter, in *Semiconductors and Semimetals*, edited by R. K. Willardson and A. C. Beer (Academic Press Inc., New York, 1967), Vol. III, p. 71.

Numbering the ions in the order Al, Ga, As, the equation of motion for the Al ions is

$$m_1\ddot{u}_1 = -k_{13}(u_1 - u_3) - (1-x)k_{12}(u_1 - u_2) + e_1 E_{\text{eff}}, \quad (1)$$

with similar expressions for the equations of motion of the Ga and As ions. In these equations, u_i represents the displacement of sublattice i with respect to its equilibrium position, m_i is the mass, and e_i is the effective charge of ion i . The elastic force constants between sublattices i and j are denoted by k_{ij} , while E_{eff} is the effective field acting upon the ion charges. In the case of compound materials, which are partly ionic and partly covalent in nature, it is impossible to consider the effective ion charge as entirely localized at the ion sites. Instead, following Burstein,¹⁰ the effective ion charges are considered as being divided into local and nonlocal fractions,

$$e_i = e_i^l + e_i^{nl}. \quad (2)$$

The nonlocal part of the effective charge is assumed to be distributed over a large number of atomic distances so that it interacts only with the macroscopic electric field E . With this assumption concerning the charge distribution, the effective field acting upon the remaining local charges in cubic symmetry sites is, for transverse vibrations,

$$E_{\text{eff}} = E + \frac{4}{3}\pi P_{\text{loc}}. \quad (3)$$

P_{loc} is the atomic displacement polarization

$$P_{\text{loc}} = N[xe_1^l u_1 + (1-x)e_2^l u_2 + e_3^l u_3], \quad (4)$$

where N is the ion pair density. The macroscopic polarization field is given by

$$P = N[xe_1 u_1 + (1-x)e_2 u_2 + e_3 u_3], \quad (5)$$

and the lattice contribution to the dielectric constant is equal to $4\pi P/E$. Substitution for the effective field terms in Eq. (1) with the aid of Eqs. (2)–(4) gives the ion displacements u_i as a function of the macroscopic field E . After this substitution is carried out, the elastic force constants k_{ij} and the dipolar force constants $\frac{4}{3}\pi N e_i^l e_j^l$ can be combined in a total or dynamic force constant

$$d_{ij} = k_{ij} + \frac{4}{3}\pi N e_i^l e_j^l,$$

and Eq. (1) can be rewritten in the form

$$m_1\ddot{u}_1 = -[d_{13} + (1-x)d_{12}]u_1 + (1-x)d_{12}u_2 + d_{13}u_3 + e_1 E. \quad (6)$$

Similar equations of motion exist for the Ga and As ions.

The transverse mode frequencies obtained by solving the equations of motion are a function only of the values of the dynamic force constants d_{ij} and masses m_i . The mode strengths and, hence, the longitudinal mode frequencies depend in addition on the values of the total effective ion charges e_i .

¹⁰ E. Burstein, in *Phonons and Phonon Interactions*, edited by T. A. Bak (W. A. Benjamin, Inc., New York, 1964), p. 276.

The general method of solving the equations of motion by diagonalizing the force constant matrix has been discussed in detail by Verleur and Barker.² The diagonalization procedure is carried out with a computer and yields the resonant transverse mode frequencies ω_{l1} , ω_{l2} and the corresponding eigenvectors and mode strengths S_1 , S_2 as a function of composition x . In this model, the force matrix is of rank 3 so that three distinct eigenfrequencies are obtained. Two eigenfrequencies represent infrared-active modes. Examination of the associated eigenvectors show that the high-frequency branch corresponds to the AlAs-like mode in the alloy and consists mainly of the vibration of the Al sublattice against the As sublattice with only a relatively small displacement of the Ga sublattice, while the low-frequency branch corresponds to the GaAs-like mode and consists of the Ga sublattice vibrating against the As and Al sublattices. The third eigenfrequency is always zero and corresponds to the $\mathbf{k}=0$ acoustic mode.

The dielectric constant for this model is given by

$$\epsilon = \epsilon_\infty + \frac{S_1 \omega_{l1}^2}{\omega_{l1}^2 - \omega^2 - i\omega\gamma_1 \omega_{l1}} + \frac{S_2 \omega_{l2}^2}{\omega_{l2}^2 - \omega^2 - i\omega\gamma_2 \omega_{l2}}, \quad (7)$$

where the two frequency-dependent terms represent the ionic contributions to the dielectric constant (with a phenomenological damping coefficient γ_i introduced *a posteriori* for each mode). The constant term is determined by noting that, at sufficiently high frequencies where the lattice modes are inactive, the dielectric constant must tend towards ϵ_∞ . The low-frequency dielectric constant is

$$\epsilon_0 = \epsilon_\infty + S_1 + S_2.$$

The longitudinal mode frequencies ω_{l1} and ω_{l2} are obtained as solutions of the equation $\epsilon=0$ assuming negligible damping ($\gamma \ll 1$).¹¹ Solution of this equation yields

$$\omega_{l1}^2 \omega_{l2}^2 = [(\epsilon_\infty + S_1 + S_2)/\epsilon_\infty] \omega_{l1}^2 \omega_{l2}^2 = (\epsilon_0/\epsilon_\infty) \omega_{l1}^2 \omega_{l2}^2 \quad (8)$$

and

$$\omega_{l1}^2 + \omega_{l2}^2 = (1 + S_1/\epsilon_\infty) \omega_{l1}^2 + (1 + S_2/\epsilon_\infty) \omega_{l2}^2. \quad (9)$$

Equations (8) and (9) are an extension of the Lyddane-Sachs-Teller relationships.

B. Determination of Force Constants and Effective Charges

The model equations that have to be solved contain seven independent parameters, namely, the nearest- and second nearest-neighbor force constants k_{13} , k_{23} , and k_{12} , the local ion charges e_1^l and e_2^l , and the total effective ion charges e_1 and e_2 for the Al and Ga ions. The charges on the As ion are fixed by charge neutrality conditions. Of these seven parameters, five (k_{13} , k_{23} ,

¹¹ A. S. Barker, Phys. Rev. **136**, A1290 (1964).

TABLE II. Mode frequencies in the pure compounds used to determine the force constants in the REI model.

GaAs ($x=0$)	TO mode	$\omega_t(\text{GaAs})=268\text{ cm}^{-1}$
	LO mode	$\omega_l(\text{GaAs})=292\text{ cm}^{-1}$
	Al local mode	$\omega_{\text{loc}}(\text{Al})=356\text{ cm}^{-1}$
AlAs ($x=1$)	TO mode	$\omega_t(\text{AlAs})=364\text{ cm}^{-1}$
	LO mode	$\omega_l(\text{AlAs})=402\text{ cm}^{-1}$
	Ga local mode	$\omega_{\text{loc}}(\text{Ga})=252\text{ cm}^{-1}$

k_{12} , e_1^l , and e_2^l) determine the TO mode frequency variation with x and the remaining two (e_1 and e_2) determine the mode strengths and, hence, the LO mode frequencies.

In order to match the TO, LO, and local-mode frequencies in the pure compounds, six conditions must be satisfied. These conditions are obtained by solving the model equation at $x=0$ (GaAs) and $x=1$ (AlAs). The procedure used in the selection of a set of model parameters that satisfies the above mentioned boundary conditions is to treat the second-neighbor force constant k_{12} as an adjustable parameter and to select its value such that the TO mode frequencies vary smoothly from their values in the pure compounds as the local modes are approached. The experimental mode-frequency values that must be matched are listed in Table II and the numerical values for the physical constants in the GaAs-AlAs system which are required in the calculations are listed in Table III.

Starting values for several of the model parameters can be obtained from available data on the pure compounds. The first-neighbor force constants can be determined from their relation to the elastic constants of the solid.¹² In the case of GaAs, the relation is

$$k_{23}=4aB_{\text{GaAs}},$$

where a is the lattice constant listed in Table III and $B_{\text{GaAs}}=0.755\times 10^{12}\text{ dyn/cm}^2$ is the bulk modulus.¹³ Application of this formula gives $k_{23}=170.7\text{ kg/sec}^2$ as listed in Table IV for the nearest-neighbor force constant. No experimental data on the elastic constants of AlAs are available. Dimensional analysis suggests, however, that for zinc-blende crystals, the elastic

TABLE III. Physical constants used in the REI-model calculations.

Mass	$m_1=26.92\text{ amu}$ $m_2=69.72\text{ amu}$ $m_3=74.91\text{ amu}$
Lattice constant ^a	$a=5.653\text{ \AA}$
Ion-pair density ^a	$N=2.22\times 10^{22}\text{ cm}^{-3}$
Dielectric constant	$\epsilon_{\infty 1}=8.5$ $\epsilon_{\infty 2}=10.9$

^a Very small difference in lattice constant (less than 0.01 Å) between GaAs and AlAs is neglected.

¹² M. Born and K. Huang, *Dynamical Theory of Crystal Lattices* (Clarendon Press, Oxford, 1964), p. 111.

¹³ G. L. Pearson and F. L. Vogel, in *Progress in Semiconductors*, edited by A. F. Gibson (Heywood and Co. Ltd., London, 1962), Vol. 6, p. 9.

TABLE IV. Force constants and ion charges used in the REI-model calculations.

Force constants:			
Nearest neighbor	Al-As	$k_{13}=170.7\text{ kg/sec}^2$	$\delta_{13}=-0.006$
	Ga-As	$k_{23}=170.7\text{ kg/sec}^2$	$\delta_{23}=+0.34$
Second-nearest neighbor	Al-Ga	$k_{12}=32\text{ kg/sec}^2$	
Effective ion charges: Al	Al	$e_1=2.12e$	$e_1^l=0.85e$
		$e_2=2.20e$	$e_2^l=0.91e$
	Ga		

constants should vary as q^2/b^4 , where q is the electronic charge and b is the distance between nearest-neighbor atoms.¹⁴ Since the lattice constants of GaAs and AlAs are practically identical, their force constants should, thus, be similar and the value $k_{13}=170.7\text{ kg/sec}^2$ was, likewise, adopted for the AlAs force constant.

Values for the local ion charges can now be determined to match the TO mode-frequency values in the pure compounds. The solution of the model equations for $x=0$ is

$$\omega_l^2(\text{GaAs})=[k_{23}-\frac{4}{3}\pi N(e_2^l)^2]/\mu_{23}$$

and, for $x=1$,

$$\omega_l^2(\text{AlAs})=[k_{13}-\frac{4}{3}\pi N(e_1^l)^2]/\mu_{13},$$

where the μ_{ij} 's represent the reduced masses. Values for the local ion charges that satisfy the above equation are $e_2^l=0.91$ and $e_1^l=0.85$ in units of the electronic charge e .

Values for the total effective ion charges e_1 and e_2 can, likewise, be obtained from the observed LO mode frequencies. The solution of the model equation for $x=0$ is

$$\begin{aligned}\omega_l^2(\text{GaAs}) &= (1+S_2/\epsilon_{\infty 2})\omega_l^2(\text{GaAs}) \\ &= \omega_l^2(\text{GaAs})+4\pi N e_2^2/\mu_{23}\epsilon_{\infty 2}\end{aligned}$$

and, for $x=1$,

$$\begin{aligned}\omega_l^2(\text{AlAs}) &= (1+S_1/\epsilon_{\infty 1})\omega_l^2(\text{AlAs}) \\ &= \omega_l^2(\text{AlAs})+4\pi N e_1^2/\mu_{13}\epsilon_{\infty 1}.\end{aligned}$$

After substituting all known values listed in Tables II and III, the results $e_1=2.12e$ and $e_2=2.20e$ are obtained.

The effective ion charges characterize to some extent the ionicity of the chemical bonds in the lattice, although the physical significance of these charge factors cannot be taken too literally in view of the simplified treatment adopted in the description of the effective electric field. With this reservation, it appears that GaAs is slightly more ionic than AlAs.

The frequency-matching conditions examined so far leave one adjustable parameter, the second-neighbor force constant k_{12} , undetermined. In general, it will

¹⁴ R. W. Keyes, *J. Appl. Phys.* **33**, 3371 (1962).

not be possible to find a value of k_{12} that will bring the calculated TO and LO mode frequencies in agreement with experiment at all intermediate compositions for both the AlAs-like and GaAs-like bands. Instead, depending on the choice for k_{12} , the calculated frequencies fall either above the experimental values for the AlAs-like mode or below the experimental values for the GaAs-like mode.

These results show that the model equations in their present form are unable to describe the experimental data and suggest that additional factors should be considered in the calculations. A better agreement between model and experiment can be obtained by assuming that the force constants between neighboring ions are composition-dependent rather than constant throughout the alloy. Such changes in the bond strength are expected to result from changes in the nearest-neighbor configurations and in the electron wavefunction distributions over neighboring ion pairs when the composition of the alloy is varied.

This observation lead Verleur and Barker, in their study of the GaAs_xP_{1-x} system,² to adopt different values for the bond strength for each of the possible nearest-neighbor configurations. In the REI model, where the differences in nearest neighbors are averaged out by using x , this observation leads to a force-constant composition dependence in the alloy of the form

$$k_{13}(x) = [1 + (1-x)\delta_{13}] \quad k_{13}(x=1)$$

and

$$k_{23}(x) = [1 + x\delta_{23}] \quad k_{23}(x=0),$$

where $k_{13}(x=1)$ and $k_{23}(x=0)$ are the force constants in pure AlAs and GaAs, respectively. A composition dependence is not introduced in the calculations for the second-neighbor force constants and the effective charges since their influence is small compared to that of the first-neighbor terms. The values of δ_{13} and δ_{23} are determined to fit the local mode frequencies and the second-neighbor force constant is selected to give a smooth variation of mode frequencies with composition. The resulting values are $k_{12} = 32$ kg/sec², $\delta_{13} = -0.006$, and $\delta_{23} = 0.34$. The increase in the Ga-As bond strength with decreasing Ga concentration is surprisingly large and should presumably be related to a possible interaction between the Ga vibrational modes and the continuum in the AlAs-phonon spectrum.

Additional information on the AlAs spectrum and a better understanding of the nature of the coupling mechanisms to the lattice are required in order to elucidate this point.

C. Comparison with Experiment

Using the values for the model parameters and physical constants listed in Tables III and IV, the TO and LO mode frequencies were calculated as a function of crystal composition and plotted as solid lines in Fig. 3 for comparison with the experimental data points derived from the Kramers-Kronig analysis. The agreement is good for the high-frequency mode at all compositions if the accuracy of the data points is taken into account. For the low-frequency modes, however, the fit is poor and the model seems to predict a somewhat smaller strength than that observed experimentally. The fit to the data can be improved either by allowing the second-neighbor force constant and the ion charges to be composition-dependent or by deviating from the linear law which was adopted to express the change in first-neighbor force constants with composition. These further improvements have not been attempted here, since it seems that the introduction of additional adjustable parameters may reduce the usefulness of the simple model and is not justified by the number and accuracy of the available experimental data.

V. SUMMARY

The lattice-vibration spectra of the GaAs-AlAs solid solutions were found to display a distinct two-mode behavior at all compositions. By a Kramers-Kronig analysis of the spectra, the mode frequencies were traced from the pure compounds, where the mode is the fundamental lattice reststrahlen mode, through to the range where the mode has become a local or impurity mode. This shift in mode frequencies has been interpreted on the basis of a REI lattice model with composition-dependent force constants, and the model was found to give a qualitatively correct picture of the data. Examination of the model parameters indicated that the Ga-As and Al-As bond strengths carry an important ionic contribution and that the strength of the Ga-As bond increases significantly as the mixed crystal composition is varied from pure GaAs to pure AlAs.